UDC 621.3 **doi: 10.20998/2074-272X.2021.1.09**

B. Ayachi, T. Boukra, N. Mezhoud

MULTI-OBJECTIVE OPTIMAL POWER FLOW CONSIDERING THE MULTI-TERMINAL DIRECT CURRENT

Introduction. *In recent years, transmission systems comprise more direct current structures; their effects on alternating current power system may become significant and important. Also, multi-terminal direct current is favorable to the integration of large wind and solar power plants with a very beneficial ecological effect. The* ***novelty*** *of the proposed work consists in the effects of the aforementioned modern devices on transient stability, thus turn out to be an interesting research issue. In our view, they constitute a new challenge and an additional complexity for studying the dynamic behavior of modern electrical systems.* ***Purpose.*** *We sought a resolution to the problem of the transient stability constrained optimal power flow in the alternating current / direct current meshed networks. Convergence to security optimal power flow has been globally achieved.* ***Methods.*** *The solution of the problem was carried out in MATLAB environment, by an iterative combinatorial approach between optimized power flow computation and dynamic simulation.* ***Results.*** *A new transient stability constrained optimal power flow approach considering multi-terminal direct current systems can improve the transient stability after a contingency occurrence and operate the system economically within the system physical bounds.* ***Practical value.*** *The effectiveness and robustness of the proposed method is tested on the modified IEEE 14-bus test system with multi-objective optimization problem that reflect active power generation cost minimization and stability of the networks. It should be mentioned that active power losses are small in meshed networks relative to the standard network. The meshed networks led to a gain up to 46,214 % from the base case.* References 24, table 3, figures 11.
Key words: **transient stability constrained optimal power flow, multi-terminal direct current.**

Вступ. *В останні роки системи передачі електроенергії включають в себе більше структур постійного струму; їх вплив на енергосистему змінного струму може стати значним і важливим. Крім того, багатотермінальний постійний струм є сприятливим для інтеграції великих вітрових та сонячних електростанцій з дуже позитивним екологічним ефектом.* ***Новизна*** *запропонованої роботи полягає у впливі вищезазначених сучасних пристроїв на перехідну стабільність, що виявляється цікавим питанням для дослідження. На наш погляд, вони становлять нову проблему та додаткову складність для вивчення динамічної поведінки сучасних електричних систем.* ***Мета****. Ми шукали розв'язання задачі перехідної стабільності, обмеженої оптимальним потоком потужності в мережах змінного/постійного струму. Збіжність для забезпечення оптимального потоку енергії була глобально досягнута.* ***Методи****. Розв'язання задачі було здійснено в середовищі MATLAB за допомогою ітеративного комбінаторного підходу між оптимізованим обчисленням потоку потужності та динамічним моделюванням.* ***Результати****. Новий підхід, що обмежує перехідну стабільність, з урахуванням багатотермінальних систем постійного струму може покращити перехідну стабільність після виникнення непередбачених ситуацій та економічно експлуатувати систему у фізичних межах системи.* ***Практичне значення.*** *Ефективність та надійність запропонованого методу перевіряється на модифікованій тестовій 14-шинній системі IEEE з використанням багатоцільової задачі оптимізації, яка відображає мінімізацію витрат на активну генерацію електроенергії та стабільність мереж.* Бібл. 24, табл. 3, рис. 11.
Ключові слова: **перехідна стабільність, обмежена оптимальним потоком потужності, багатотермінальний постійний струм.**

Introduction. In a competitive economic environment that has placed the need for reconciliation of economic and transitional stability conditions, the cost of losing synchronism by transient instability is exceptionally high and of significant importance. For this reason, the traditional optimal power flow (OPF) approach has been extended to take into account the transient stability constraints of the system, giving a new transient stability constrained optimal power flow (TSC-OPF) approach [1]. The TSC-OPF procedures are classified in either global or sequential approaches [2, 3]. The global TSC-OPF approaches are reported in [4-7]. The sequential TSC-OPF approaches perform a standard OPF analysis to assess an optimal operating point [1]. A transient stability analysis is then carried out independently from the optimization process to check if the optimum point is transiently stable, so that the time domain simulation-related set of differential algebraic equations is not embedded in the traditional OPF problem [2, 8-10]. In recent decades, various optimization approaches have been proposed [11]. Among them, those dedicated to solve the multi-objective TSC-OPF problems where different goals and different constraints have been taken into account [12-14].

A proposed network topology in [15-18] has been used in our work for simulations propose. The meshed topology is of great interest for our proposed methodology.

This paper is organized as follows: first part concerns modelling AC/DC power system. In the second part, the TSC-OPF problem has been formulated. In the third part, the experimental results and conclusions are presented.

AC/DC power system modelling. A generalized AC/DC system of Fig. 1 consists of three parts.

1. AC grid. We present here the expressions for active and reactive power injections. Reader may refer to [19] for more details:

$$P_{gi}^{AC} = \sum_{j=1}^{n} \left|V_i^{AC}\right| \cdot \left|V_j^{AC}\right| \cdot \left(G_{ij}\cos\delta_{ij} + B_{ij}\sin\delta_{ij}\right); \quad (1)$$

$$Q_{gi}^{AC} = \sum_{j=1}^{n} \left|V_i^{AC}\right| \cdot \left|V_j^{AC}\right| \cdot \left(G_{ij} \sin \delta_{ij} - B_{ij} \cos \delta_{ij}\right), \quad (2)$$

where P_{gi}^{AC}, Q_{gi}^{AC} are active and reactive power generations at bus i respectively; V_i^{AC}, V_j^{AC} are nodal voltage values at buses i and j respectively; δ_{ij} is angle voltage of unit i and j; G_{ij} is the conductance; B_{ij} is the susceptance; n is the total number of generators.

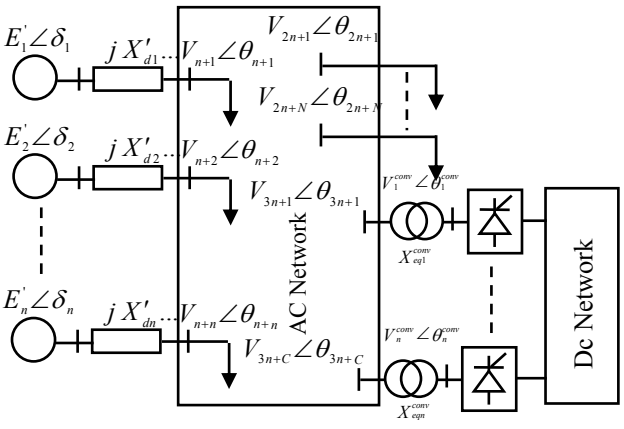

Fig. 1. Model for combined AC and DC grid

2. HVDC converters. Assuming a lossless converter model. The active power of the AC side converter coincides with that of the DC side:

$$P_c^{AC} = P_c^{DC}. \quad (3)$$

An HVDC converter station was modeled as a voltage source with variable value V^{conv} and angle θ^{conv} connected to an AC bus via a reactance X_{eq}^{conv}. By varying the voltage source, it is possible to produce the desired active and reactive power flow from the DC to the AC network or vice versa

$$P_i^{DC} = \frac{V_i^{AC} \cdot V_i^{conv}}{X_{eq}^{conv}} \sin\left(\theta_i^{AC} - \theta_i^{conv}\right); \quad (4)$$

$$Q_i^{DC} = \frac{V_i^{2,AC}}{X_{eq}^{conv}} - \frac{V_i^{AC} \cdot V_i^{conv}}{X_{eq}^{conv}} \cos\left(\theta_i^{AC} - \theta_i^{conv}\right). \quad (5)$$

3. DC grid. The power flows over the DC lines can be calculated as follows:

$$P_{ij}^{DC} = \frac{V_i^{DC} - V_j^{DC}}{R_{ij}}. \quad (6)$$

Problem statement and formulation. The theory of TSC-OPF is an extension of the standard OPF problem to include supplementary constraints for imaginable credible contingencies cases. In a standard form, the OPF problem is defined as in [20-22]:

$$\min f(x,u), \quad (7)$$

subject to

$$h(x,u) = 0; \quad (8)$$

$$g(x,u) \le 0. \quad (9)$$

where x is a vector of state variables; u is a vector of control variables; h, g are functions; $f(x, u)$ is an objective function.

In general, the intention is to minimize the objective function with the solution satisfying a number of equality and inequality constraints. But the TSC-OPF problem can be mathematically considered as a standard OPF with other inequality dynamic constraints forced by the rotor angles of generators during the transient period in study for a given set of contingencies.

1. Objective function. The objective functions f of TSC-OPF is minimization of fuel cost for all generators:

$$f = \min \sum_{i=1}^{n_g} \left(a_i + b_i \cdot P_{gi} + c_i \cdot P_{gi}^2\right), \quad (10)$$

where n_g is number of generators; a_i, b_i, c_i, are cost coefficients of unit i; P_{gi} is an active power generations by unit i.

2. Equality constraints. The equality constraints $h(x, u)$ are the sets of the load flow equations that govern the power system:

$$P_{gi}^{AC} + P_i^{DC} - P_{di} = 0; \quad (11)$$

$$Q_{gi}^{AC} + Q_i^{DC} - Q_{di} = 0, \quad (12)$$

where P_{di}, Q_{di} are active and reactive power loads by unit i respectively.

3. Inequality constraints (standard OPF). The inequality constraints $g(x, u)$ are the set of constraints that represent the system operational and security bounds like the limits on the following:

$$P_{AC,gi}^{\min} \le P_{gi} \le P_{AC,gi}^{\max}; \text{ where } i = 1,..., n_g; \quad (13)$$

$$Q_{AC,gi}^{\min} \le Q_{gi} \le Q_{AC,gi}^{\max}; \text{ where } i = 1,..., n_g; \quad (14)$$

$$V_{AC,i}^{\min} \le V_i \le V_{AC,i}^{\max}; \ \ i = 1,....., n_b; \quad (15)$$

$$\theta_i^{\min} \le \theta_i \le \theta_i^{\max}; \ \ i = 1,....., n_b; \quad (16)$$

$$T_i^{\min} \le T_i \le T_i^{\max}; \ \ i = 1,....., n_T, \quad (17)$$

where $P_{AC,gi}^{\min}, P_{AC,gi}^{\max}$ and $Q_{AC,gi}^{\min}, Q_{AC,gi}^{\max}$ are the lower and upper limits of active and reactive power generation at bus i of AC network respectively; Q_{gi} is reactive power generations at bus i; $V_{AC,i}^{\min}, V_{AC,i}^{\max}$ are the lower and upper limits of voltage value at buses i; V_i is voltage value at buses i; n_b is total number of buses; $\theta_i^{\min}, \theta_i^{\max}$ are the lower and upper limits of angle voltage; θ_i is the angle voltage of unit i; $T_i^{\min}, T_i^{\max}$ are the lower and upper limits of transformers tap settings; T_i is transformers tap settings of unit i; n_T is total number of transformers.

4. Inequality constraints (transient stability). The transient stability problem in power system is defined by a differential algebraic equation, which can be solved by time domain simulation. The swing equation for i^{th} generators is:

$$\frac{d\omega_i}{dt} = \frac{\omega_i}{M_i}\left[\left(P_{mi} - P_{ei}\right) - D\left(\omega_s - \omega_i\right)\right]; \quad (18)$$

$$\frac{d\delta_i}{dt} = \omega_i - \omega_s; \text{ where } i = 1,.....,n_g \quad (19)$$

$$\frac{dE'_{di}}{dt} = \frac{1}{T'_{qi0}}\left[-E'_{di} + (X_{qi} - X'_{qi})i_{qi}\right]; \quad (20)$$

$$\frac{dE'_{qi}}{dt}=\frac{1}{T'_{di0}}\left[E_{fdi}-E'_{qi}-(X_{di}-X'_{di})i_{di}\right]; \quad (21)$$

$$\frac{dE_{fdi}}{dt}=\frac{1}{T_{Ai}}\left[-E_{fdi}+K_{Ai}(V_{refi}-V_t)\right]; \quad (22)$$

$$\frac{d\omega_i}{dt}=\frac{\omega_i}{M_i}\left[(P_{mi}-P_{ei})-D(\omega_s-\omega_i)\right]; \quad (23)$$

$$\frac{d\delta_i}{dt}=\omega_i-\omega_s, \text{ where } i=1,.....,n_g, \quad (24)$$

where P_{mi} is the mechanical input generator by unit i; P_{ei} is the electrical output generator by unit i; M_i is the moment of inertia of i^{th} generator; ω_i is the angular speed of the rotating synchronous reference frame of unit i; ω_s is the angular speed of the generator rotor of unit i; δ_i is rotor angle of unit i; D is the generators damping torque coefficient; E'_{di}, E'_{qi} are the internal transient voltage of generator of unit i; E_{fdi} is the excitation voltage of generator of unit i; i_{di}, i_{qi} are d-axis and q-axis courant of generator of unit i; T'_{d0i}, T'_{q0i} are the d-open circuit and q-open circuit transient time constants of generator of unit i; X'_{di}, X'_{qi} are the d-transient reactance and q-transient reactance of generator of unit i; X_{di}, X_{qi} are the d-synchronous reactance and q-synchronous reactance of generator of unit i; V_{refi} is voltage reference of generator of unit i.

The inequality constraints of transient stability are formulated as:

$$\left|\delta_i-\delta_{COI}\right|\le\delta_{\max}; \quad (25)$$

$$\delta_{COI}=\frac{\sum_{i=1}^{n_g}M_i\delta_i}{\sum_{i=1}^{n_g}M_i}, \quad (26)$$

where δ_i is the rotor angle of unit i; δ_{COI} is the position angle of centre of inertia (COI – centre of inertia); $\delta_{\max}$ is the maximum allowable rotor angle deviation

The selection of $\delta_{\max}$ is frequently based on experiment operation. It was generally limited to 100° to allow network having sufficient stability margin [23, 24].

5. Inequality constraints (multi-terminal direct current – MTDC). The last constraint limits the variance of the all DC nodes have their minimal and maximal voltage angle limits, in which the equipment can operate safely.

$$\theta^{\min}_{DC,j}\le\theta_{DC,j}\le\theta^{\max}_{DC,j}; \text{ where } j=1,.....,n_{b'}; \quad (27)$$

$$P^{\min}_{DC,j}\le P_{DC,j}\le P^{\max}_{DC,j}; \text{ where } j=1,.....,n_{b'}, \quad (28)$$

where $P^{\min}_{DC,j}, P^{\max}_{DC,j}$ are the lower and upper limits of active power generation at bus j of DC buses; P_{DCj} is the active power generation at bus j of DC buses; $\theta^{\min}_{DC,j}, \theta^{\max}_{DC,j}$ are the lower and upper limits of angle voltage of DC buses; θ_{DCj} is the angle voltage of DC buses; $n_{b'}$ is the total number of DC buses.

Simulation results and discussion. In this paper, the MTDC system presented for the simulation with integrated offshore wind farm is shown in Fig. 2. This system is a modified version of the IEEE 14-bus test system. A meshed DC grid including an additional generator has been added, that connects to the AC system to various buses through voltage source converters (VSC). The bus 19 is not connected to any VSC. The bus and line parameters were given in the [24]. All the simulations were performed on source codes developed in MATLAB environment running on an Intel Core i5 2.67GHz CPU and 3GB RAM.

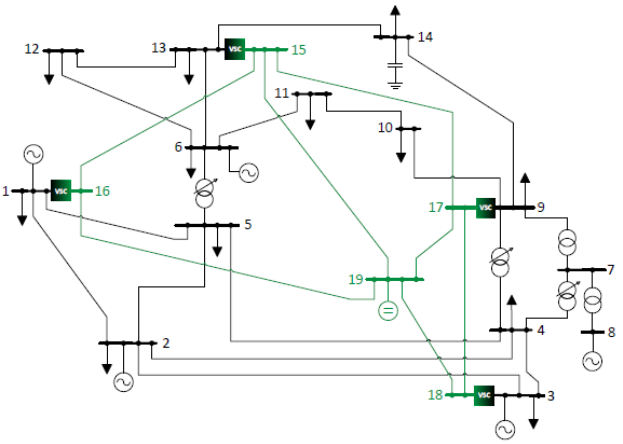

Fig. 2. Modified IEEE 14-bus

The fault priority list was given in Table 1. The top 4 faults in critical clearing time (CCT) are considered.

According to Table 1 and Fig. 3, it is evident that the most unfavorable case is the three-phase fault (3φ). However, it should be noted that there are, for certain types of connection, cases where other types of fault are more damaging. The best known of these faults are:

- single line to ground fault (SLG), when the generator neutral is connected to ground directly or through low impedance;
- single line to ground fault, when the transformer is connected in Y-Δ with neutral grounded.

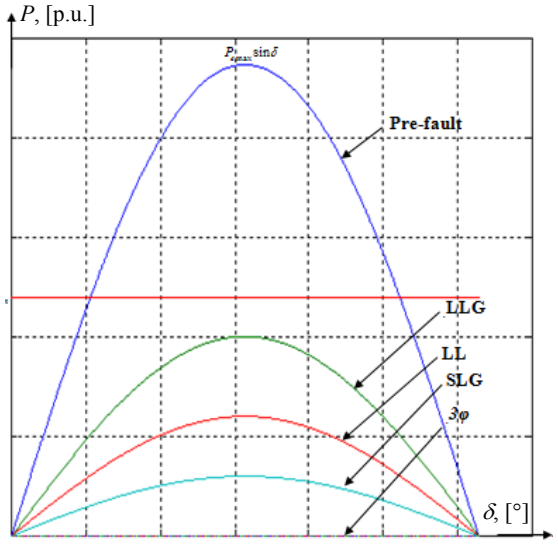

Fig. 3. Power injected by the generator, depending on the type of fault (LLG is double line to ground fault; LL is line to line faults; SLG is single line to ground fault; 3φ is three-phase fault)

Table 1

Priority list of fault for IEEE 14 bus system

Cases	Faults		Line	CCT(s)
	3φ	SLG		
1	1		1-2	0.33
2	1		1-5	0.36
3		1	1-2	0.38
4	2		1-2	0.40

The severity criteria considered in this study is the critical clearing time (CCT). This study was performed according to the 2 different faults (three-phase fault and single line to ground).

In this section, the modified IEEE 14-bus system has been used to illustrate the effectiveness of the proposed method. There are 5 cases to be discussed here, each with 2 scenarios:

- Case 1 is the standard power flow (PF);
- Case 2 is the standard OPF without transient stability constraints;
- Case 3 is OPF with transient stability constraints;
- Case 4 when IEEE 14-bus is modified, with added MTDC and without transient stability constraints;
- Case 5 using a new configuration of network with transient stability constraints.

The results are given in Table 2.

Table 2

Optimization results for IEEE 14 bus system

	Case 1		Case 2		Case 3		Case 4		Case 5	
	3φ fault	SLG fault	3φ fault	SLG fault	3φ fault	SLG fault	3φ fault	SLG fault	3φ fault	SLG fault
P_{g1}, MW	232		194.41		186.63	174.97	146.41		137.63	120.06
P_{g2}, MW	40		36.74		37.03	37.44	25.61		34.34	39.61
P_{g3}, MW	0		28.61		31.53	35.41	0		0	0.07
P_{g6}, MW	0		0		0	1.28	0		0	8.82
P_{g8}, MW	0		8.52		12.44	17.58	0		0	3.23
P_{g19}, MW	–		–		–	–	100		100	100
Fuel cost ($/h)	–		8080.77		8084.20	8102.18	5526.65		5549.29	5691.48
CCT (s)	0.33	0.38	0.51	0.45	0.57	0.47	0.28	0.37	0.31	0.39
Losses (MW)	–		9.277		8.610	7.674	1.417		1.370	1.187

First, simulation results were presented with standard PF (case 1). With this generation, it was found that system transient stability was lost following the three-phase fault disturbance at bus 1 (cleared by tripping line 1-2 at 0.33 s), and was lost following single line to ground fault at bus 1 (cleared by tripping line 1-2 at 0.38 s) respectively. Visibly the system can't operate under this mode.

The second simulation (case 2), was the standard OPF without transient stability constraints; the objective function (fuel cost) reached 8080.77 $/h. But with this generation, it was found that system transient stability was lost following the fault disturbance at bus 1, as shown in Fig. 4, 5, respectively. Visibly the system can't operate under this mode because security of the network is always violated.

Case 3, scenario 1 (3φ fault), the active power of generator 1 is reduced from 194.41 MW to 186.63 MW, while those of generators 2, 3 and 8 were increased from 36.74 MW, 28.61 MW and 8.52 MW (case 2) to 37.44 MW, 31.53 MW and 12.44 MW (case 3) respectively. A fuel cost was increased from 8080.77 $/h (case 2) to 8084.20 $/h (case 3) as shown in Table 2 and Fig. 6. A consequence of satisfying the transient stability constraints is the increasing in fuel cost only by 0.042 %.

For scenario 2 (SLG fault), the active power of generator 1 is reduced from 194.41 MW to 174.97 MW. While those of generators 2, 3, 6 and 8 were increased from 36.74 MW, 28.61 MW, 0 MW and 08.52 MW to 37.44 MW, 35.41 MW, 1.28 MW and 17.58 MW (case 3) respectively. The fuel cost was increased from 8080.77 $/h (case 2) to 8102.18 $/h (case 3) as shown in Table 2 and Fig. 7. A consequence of satisfying the transient stability constraints is the increasing in fuel cost only by 0.246 %.

From Fig. 6, 7, the use of transient stability constraints in terms of OPF solution gives better results and ensures system transient stability following the fault disturbances.

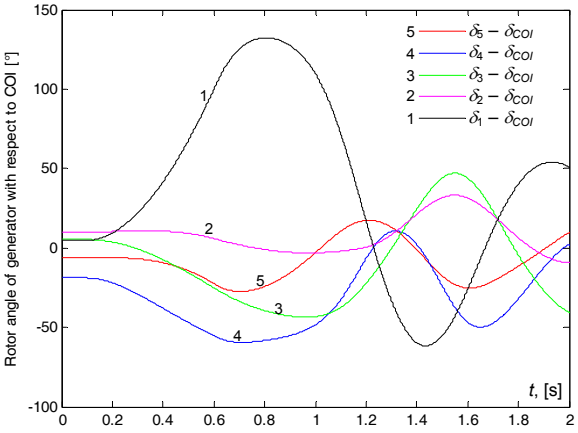

Fig. 4. Response of rotor angle (case 2, OPF), 3φ fault

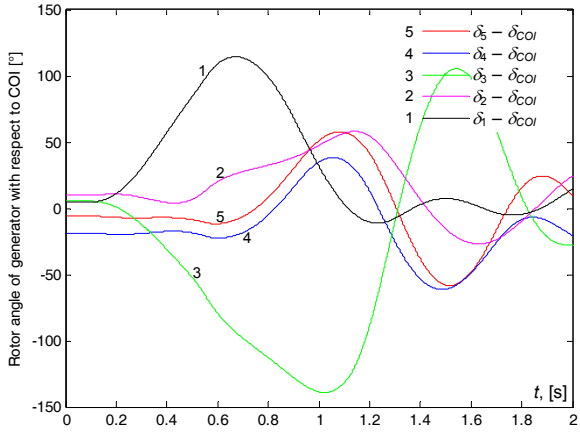

Fig. 5. Response of rotor angle (case 2, OPF), SLG fault

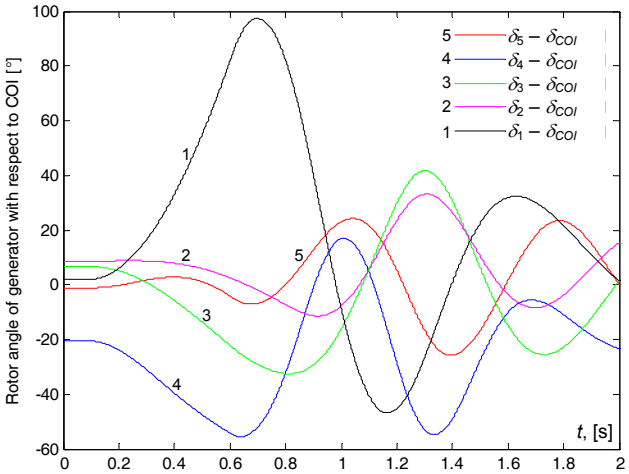

Fig. 6. Response of rotor angle (case 3, TSC-OPF), 3φ fault

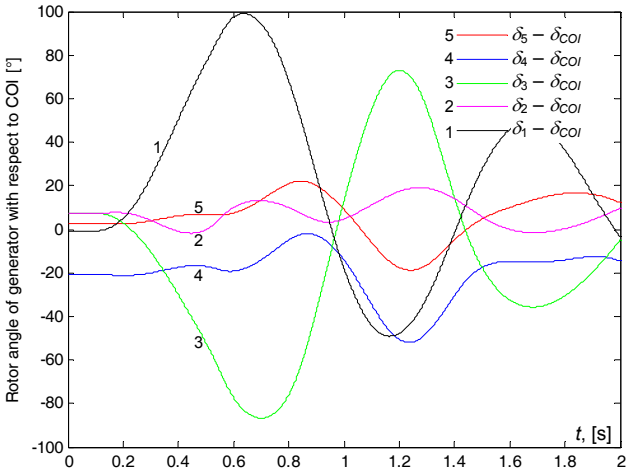

Fig. 7. Response of rotor angle (case 3, TSC-OPF), SLG fault

Cases 4 and 5 the network is modified, and at the present the total loads is 295 MW (new load at bus 1, active power 11.6 MW) and a new generator is present on the DC bus (bus 19). The solution of cases 4 and 5, with and without transient stability constraints is given in Table 2.

The fourth simulation (case 4), the fuel cost was reduced to 5526.66 $/h. But with this generation, it was found that system transient stability was lost following the fault disturbance at bus 1, as shown in Fig. 8, 9, respectively. Visibly the system can't operating under this mode because security of the network was violated.

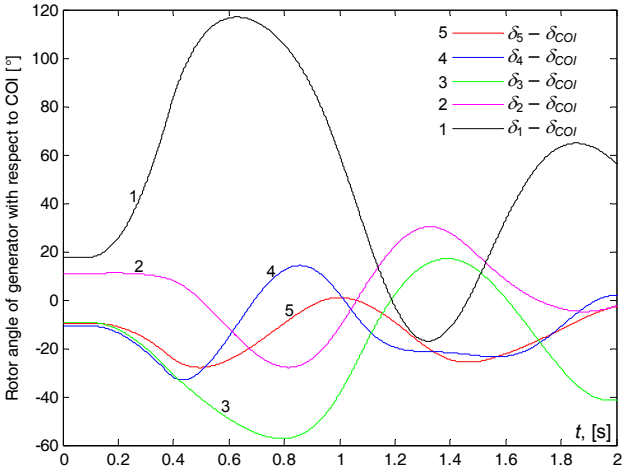

Fig. 8. Response of rotor angle (case 4, OPF, MTDC), 3φ fault

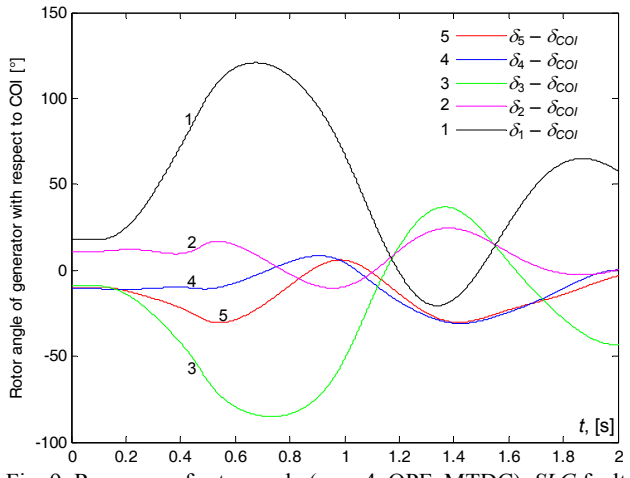

Fig. 9. Response of rotor angle (case 4, OPF, MTDC), *SLG* fault

In case 5, scenario 1 (3φ fault), in order to retain the transient stability limits, the active power of generator 1 was reduced from 146.41 MW to 137.63 MW, while that of generator 2 was increased to 34.34 MW. The fuel cost was increased from 5526.66 $/h to 5549.29 $/h as shown in Table 1 and Fig. 8. A consequence of satisfying the transient stability constraints was the increase in fuel cost by 0.409 %.

For last scenario (SLG fault), the active power of generator 1 is reduced to 120.06 MW. While those of generators 2, 3, 6 and 8 were increased to 39.61 MW, 0.07 MW, 8.82 MW and 3.23 MW, respectively. A consequence of satisfying the transient stability constraints was the increase in fuel cost by 2.982 %.

From Fig. 10, 11 it was obvious that the use of TSC in OPF solution gives better results and guarantees transient stability following the fault.

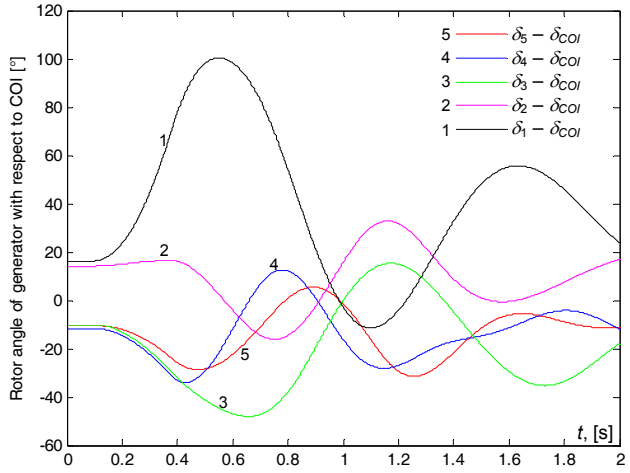

Fig. 10. Response of rotor angle (case 5, TSC-OPF, MTDC), 3φ fault

For the best compromise solution, we must maintain a balance between stability and economy. The solution obtained enhances the transient stability of the system at the best acceptable cost. Generally, in this situation, the cost is marginally higher as the economy is sacrificed for the improvement of transient stability. In case of lower cost solution, more emphasis is given to economy of the system and this solution is unable to improve the global transient stability of the network. For minimum cost

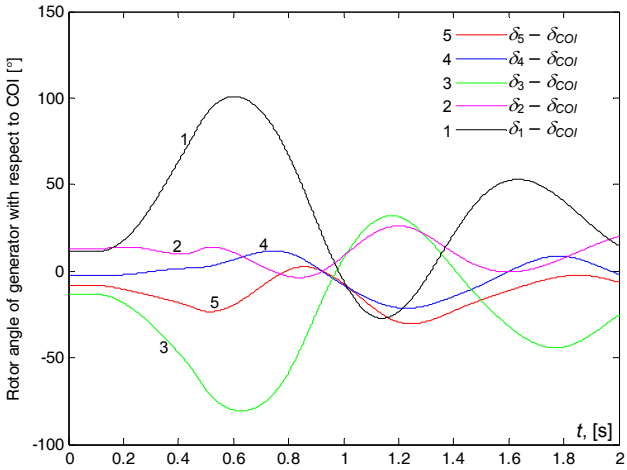

Fig. 11. Response of rotor angle (case 5, TSC-OPF, MTDC), SLG fault

case 4, the CCT for the fault at bus 1 cleared by tripping line 1-2 becomes 0.28 s whereas it was 0.33 s for three-phase fault and 0.37 s to 0.38 s for base case for single line to ground fault, as shown in Table 3.

Table 3

CCT comparison

	3φ fault	SLG fault
Case 1	0.33	0.38
Case 2	0.51	0.45
Case 3	0.57	0.47
Case 4	0.28	0.37
Case 5	0.31	0.39

Finally, the solution sought for the problem of the transient stability constrained optimal power flow, in the last case, compared to all the previous solutions that maximize the transient stability index, has the highest cost as more focus is placed on optimizing the system's transient efficiency. In the event of emergency situations, this approach can be extremely useful.

It should be mentioned that active power losses are small in mixed AC/DC networks relative to the standard AC network. The AC/DC networks led to a gain up to 46,214 % from the base case. This confirms the potential need for construction of solar or wind farms, considering their advantages.

Conclusions.

It is very likely that future transmission systems will contain more multi-terminal direct current links and the effects of such system on transient stability are yet to be determined. The increase of the future system has led to a growing complexity in the study of its problem and so presents new defy to power system stability. This paper suggests a new version of the multi-objective optimal power flow, taking into account the transient stability of the power system. Two goals were concurrently considered; minimizing the cost of the fuel and optimizing the system's transient stability margin at the point of fault clearance. Furthermore, this study was performed on the basis of two different faults namely three-phase fault and single line to ground fault.

Simulations were carried out in MATLAB environment, the transient stability of the system is compared with and without the presence of transient stability constraints. The use of transient stability constraints in terms of optimal power flow solution gives better results and also ensures system transient stability following the fault disturbance.

Conflict of interests. The authors declare no conflicts of interest.

REFERENCES

1. Pizano-Martinez A., Fuerte-Esquivel C.R., Zamora-Cardenas E.A., Lozano-Garcia J.M. Directional Derivative-Based Transient Stability-Constrained Optimal Power Flow. *IEEE Transactions on Power Systems*, 2017, vol. 32, no. 5, pp. 3415-3426. doi: https://doi.org/10.1109/tpwrs.2016.2633979.

2. Nguyen T.B., Pai M.A. Dynamic security-constrained rescheduling of power systems using trajectory sensitivities. *IEEE Transactions on Power Systems*, 2003, vol. 18, no. 2, pp. 848-854. doi: https://doi.org/10.1109/tpwrs.2003.811002.

3. Tu X., Dessaint L., Kamwa I. A global approach to transient stability constrained optimal power flow using a machine detailed model. *Canadian Journal of Electrical and Computer Engineering*, 2013, vol. 36, no. 1, pp. 32-41. doi: https://doi.org/10.1109/cjece.2013.6544470.

4. Gan D., Thomas R.J., Zimmerman R.D. Stability-constrained optimal power flow. *IEEE Transactions on Power Systems*, 2000, vol. 15, no. 2, pp. 535-540. doi: https://doi.org/10.1109/59.867137.

5. La Scala M., Trovato M., Antonelli C. On-line dynamic preventive control: an algorithm for transient security dispatch. *IEEE Transactions on Power Systems*, 1998, vol. 13, no. 2, pp. 601-610. doi: https://doi.org/10.1109/59.667388.

6. Pizano-Martinez A., Fuerte-Esquivel C.R., Ruiz-Vega D. Global Transient Stability-Constrained Optimal Power Flow Using an OMIB Reference Trajectory. *IEEE Transactions on Power Systems*, 2010, vol. 25, no. 1, pp. 392-403. doi: https://doi.org/10.1109/tpwrs.2009.2036494.

7. Zarate-Minano R., Van Cutsem T., Milano F., Conejo A.J. Securing Transient Stability Using Time-Domain Simulations Within an Optimal Power Flow. *IEEE Transactions on Power Systems*, 2010, vol. 25, no. 1, pp. 243-253. doi: https://doi.org/10.1109/tpwrs.2009.2030369.

8. Ruiz-Vega D., Pavella M. A comprehensive approach to transient stability control. I. Near optimal preventive control. *IEEE Transactions on Power Systems*, 2003, vol. 18, no. 4, pp. 1446-1453. doi: https://doi.org/10.1109/tpwrs.2003.818708.

9. Bettiol A.L., Wehenkel L., Pavella M. Transient stability-constrained maximum allowable transfer. *IEEE Transactions on Power Systems*, 1999, vol. 14, no. 2, pp. 654-659. doi: https://doi.org/10.1109/59.761894.

10. Pizano-Martinez A., Fuerte-Esquivel C.R., Ruiz-Vega D. A New Practical Approach to Transient Stability-Constrained Optimal Power Flow. *IEEE Transactions on Power Systems*, 2011, vol. 26, no. 3, pp. 1686-1696. doi: https://doi.org/10.1109/tpwrs.2010.2095045.

11. Ghasemi M., Ghavidel S., Ghanbarian M.M., Gharibzadeh M., Azizi Vahed A. Multi-objective optimal power flow considering the cost, emission, voltage deviation and power losses using multi-objective modified imperialist competitive algorithm. *Energy*, 2014, vol. 78, pp. 276-289. doi: https://doi.org/10.1016/j.energy.2014.10.007.

12. Yue Yuan, Kubokawa J., Sasaki H. A solution of optimal power flow with multicontingency transient stability constraints. *IEEE Transactions on Power Systems*, 2003, vol. 18, no. 3, pp. 1094-1102. doi: https://doi.org/10.1109/tpwrs.2003.814856.

13. Xu Y., Dong Z.Y., Meng K., Zhao J.H., Wong K.P. A Hybrid Method for Transient Stability-Constrained Optimal

Power Flow Computation. *IEEE Transactions on Power Systems*, 2012, vol. 27, no. 4, pp. 1769-1777. doi: https://doi.org/10.1109/tpwrs.2012.2190429.
14. Ye C.-J., Huang M.-X. Multi-Objective Optimal Power Flow Considering Transient Stability Based on Parallel NSGA-II. *IEEE Transactions on Power Systems*, 2015, vol. 30, no. 2, pp. 857-866. doi: https://doi.org/10.1109/tpwrs.2014.2339352.
15. Saplamidis V., Wiget R., Andersson G. Security constrained Optimal Power Flow for mixed AC and multi-terminal HVDC grids. *2015 IEEE Eindhoven PowerTech*, Eindhoven, 2015, pp. 1-6. doi: https://doi.org/10.1109/ptc.2015.7232616.
16. Wiget R., Vrakopoulou M., Andersson G. Probabilistic security constrained optimal power flow for a mixed HVAC and HVDC grid with stochastic infeed. *2014 Power Systems Computation Conference*, Wroclaw, 2014, pp. 1-7. doi: https://doi.org/10.1109/pscc.2014.7038408.
17. Wiget R., Iggland E., Andersson G. Security constrained optimal power flow for HVAC and HVDC grids. *2014 Power Systems Computation Conference*, Wroclaw, 2014, pp. 1-7. doi: https://doi.org/10.1109/pscc.2014.7038444.
18. Wiget R., Andersson G. Optimal power flow for combined AC and multi-terminal HVDC grids based on VSC converters. *2012 IEEE Power and Energy Society General Meeting*, San Diego, CA, 2012, pp. 1-8. doi: https://doi.org/10.1109/pesgm.2012.6345448.
19. Duong T., JianGang Y., Truong V. Improving the transient stability-constrained optimal power flow with Thyristor Controlled Series Compensators. *Russian Electrical Engineering*, 2014, vol. 85, no. 12, pp. 777-784. doi: https://doi.org/10.3103/s1068371214120165.
20. Acha E., Roncero-Sánchez P., Villa Jaén A., Castro L.M., Kazemtabrizi B. *VSC-FACTS-HVDC Analysis, Modelling and Simulation in Power Grids*. JohnWiley & Sons Ltd Publ., 2019. 404 p. doi: https://doi.org/10.1002/9781119190745.
21. Mukherjee A., Roy P.K., Mukherjee V. Transient stability constrained optimal power flow using oppositional krill herd algorithm. *International Journal of Electrical Power & Energy Systems*, 2016, vol. 83, pp. 283-297. doi: https://doi.org/10.1016/j.ijepes.2016.03.058.
22. Bilel A., Boukadoum A., Leulmi S., Boukra T. Improving the Transient Stability of the Mixed AC/DC Networks with FACTS. *Indonesian Journal of Electrical Engineering and Informatic*), 2018, vol. 6, no. 4, pp. 477-485. doi: https://doi.org/10.11591/ijeei.v6i4.473.
23. Abido M.A., Waqar Ahmed M. Multi-objective optimal power flow considering the system transient stability. *IET Generation, Transmission & Distribution*, 2016, vol. 10, no. 16, pp. 4213-4221. doi: https://doi.org/10.1049/iet-gtd.2016.1007.
24. Ayachi B. *Apport des FACTS intelligents à l'amélioration de la stabilité transitoire des réseaux électriques*. Doctoral thesis of 20 Aout 1955 Skikda University, 2019. Ref D012120003D. (Fra).

Received 04.11.2020
Accepted 11.12.2020
Published 25.02.2021

Bilel Ayachi[1], *Ph.D. of Power Engineering,*
Tahar Boukra[1], *Ph.D. of Power Engineering,*
Nabil Mezhoud [1], *Ph.D. of Power Engineering,*
[1] Electrotechnical Laboratory Skikda (LES),
Department of Electrical Engineering,
University 20 August 1955,
26 Road El Hadaiek 21000, Skikda, Algeria,
e-mail: b.ayachi@univ-skikda.dz,
boukratahar@hotmail.com,
mezhounab@yahoo.fr

How to cite this article:
Ayachi B., Boukra T., Mezhoud N. Multi-objective optimal power flow considering the multi-terminal direct current. *Electrical Engineering & Electromechanics*, 2021, no. 1, pp. 60-66. **doi: 10.20998/2074-272X.2021.1.09.**